J. At. Mol. Sci.
doi: 10.4208/jams.072215.082315a

Vol. **6**, No. 3, pp. 164-171
September 2015

The weakening or enhancing of N-H···O intermolecular hydrogen bond in different solvents revealed by density functional calculations

Donglin Li, and Yufang Liu*

College of Physics and Electronic Engineering, Henan Normal University, Xinxiang 453007, China

Received 22 July 2015; Accepted (in revised version) 23 August 2015
Published Online 30 September 2015

Abstract. Time-dependent density functional theory (TDDFT) method has been performed to investigate the properties of N_1-$H_1\cdots O_1$ hydrogen bond of N-methylaniline-DMSO complex (complex I) and N-methylaniline-acetone complex (complex II) in the excited state. The infrared spectra are in good agreement with the experiment data. The analysis of the bond length and AIM (atoms in molecules) demonstrated that the N_1-$H_1\cdots O_1$ hydrogen bond is weakening from DMSO to acetone in the ground state. That is to say, the intermolecular hydrogen bond N_1-$H_1\cdots O_1$ between N-methylaniline and solvent molecular is stronger with the polarity of solvent stronger. Upon photoexcitation, the analysis of AIM implies that the intermolecular complex II is enhanced. Interestingly, the hydrogen bond N_1-$H_1\cdots O_1$ of complex I is weakened. The analysis of molecular orbital also support the results that the intermolecular hydrogen bond N_1-$H_1\cdots O_1$ of complex I is weakened whereas it of complex II is enhanced.

PACS: 33.15.Fm

Key words: hydrogen bond; electrostatic potential; AIM; N-methylaniline; DFT.

1 Introduction

Hydrogen bonding has been studied by diverse experimental and theoretical methods because it is central to understanding the microscopic structure and the function of many molecular systems, such as proteins and DNA building blocks of the life [1-7]. As a site-specific solute-solvent interaction, the intermolecular hydrogen bonds between hydrogen donor and acceptor have a remarkable influence on the photophysics and photochemistry of chromophores in the hydrogen-bonding surroundings [8-12]. The hydrogen

*Corresponding author. *Email address:* yf-liu@htu.cn (Y. F. Liu)

bonding is also associated with many process including the internal conversion (IC), photoinduced electron transfer (PET), fluorescence quenching (FQ), intramolecular charge transfer (ICT) and so on [13].

Nibbering *et al.* investigated the nature of N-H···O hydrogen bond in DMSO and acetone solvents, and experimentally observed the notion of weakening the N-H···O hydrogen bond from DMSO to acetone in the ground state [14]. However, the nature of hydrogen bond and its impact factors upon photoexcitation have not been explained. As we all know, the excited state hydrogen bond strengthening theory has been used to explain many photochemistry and photophysics reactions, such as fluorescence quenching, intermolecular charge transfer, and so forth. It is well known that theoretical calculation for excited states is a reliable tool to study the excited state hydrogen bonding dynamics. Therefore, the detailed investigations of N-H···O hydrogen bond of complexes I and II in the S_1 state have been performed in this work.

In this work, the geometry structures of complexes I and II have been optimized both in the ground and excited states. The analysis of electrostatic potential is performed to confirm the reasonableness of the composed conformations and to determine the reactive sites of the reactants. The electronic excitation energies, oscillation strengths and infrared spectra of the electronically excited states are investigated to deeply analyze the nature of hydrogen bond. More importantly, the detailed theoretical investigations of the molecular structure, spectral properties and frontier molecular orbital of complexes I and II are performed. In addition, the AIM analysis has been performed to investigate the strength and types of hydrogen bonds.

2 Theoretical methods

The geometry optimizations for the ground state and the first singlet electronic excited state were performed using density functional theory (DFT) and TDDFT methods, respectively [15-17]. B3LYP functional (Becke's three-parameter hybrid exchange functions with Lee-Yang-Parr gradient-corrected correlation functional) was used in both the DFT and TDDFT methods. The TDDFT/B3LYP was used to calculate the excited states with the 6-311++G(d,p) basis set [18, 19]. All the electronic structure and spectra calculations were carried out using the G09 program suit. To account for the solvent effects, the equilibrium continue polarizable continuum model (CPCM) is used.

Bader's quantum theory of atoms in molecules (QTAIM) is an effective method for the analysis of electron density distribution in molecular systems [20]. The descriptors of charge density (ρ(r)), Laplacian of the charge density ($\nabla^2\rho$(r)) and potential energy density (V(r)) not only can be used to assess the interaction strength but also can be used to distinguish between different kinds of non-covalent interactions. Hunt and coworkers have proposed the different sets of hydrogen bonding criteria and types [21]. AIM analysis is also carried out at the B3LYP/6-311++G(d,p) level.

3 Results and discussion

3.1 The nature of hydrogen bond in ground state

3.1.1 The analysis of electrostatic potential

As well know, the electrostatic potential (ESP) model is an effective method to confirm the reasonableness of the composed conformations and to determine the reactive sites of the reactants [22, 23]. Therefore, the electrostatic potential models of DMSO, NMA and acetone molecular have been calculated as shown in Fig. 1. According to the conventional color spectrum in ESP maps, the red color represents the negative electrostatic potential whereas the blue color represents the positive electrostatic potential. As shown in the Fig. 1, for DMSO molecule, the negative charge is concentrated on the oxygen atom of carbonyl group and the positive electrostatic potential is located at methyl group. Similarly, for acetone molecular, the red regions are entirely concentrated on the oxygen atom of carbonyl group and the blue regions are totally localized on methyl group. Moreover, for NMA molecular, the N-H group is covered by blue which exhibits a local positive electrostatic potential and the red which exhibits a local negative electrostatic potential is concentrated on the benzene regions. The ESP analysis indicated that the intermolecular hydrogen bond can be formed between the N-H group of NMA and oxygen atom of carbonyl group of DMSO. The intermolecular hydrogen bond also can be formed between the N-H group of NMA and acetone molecular.

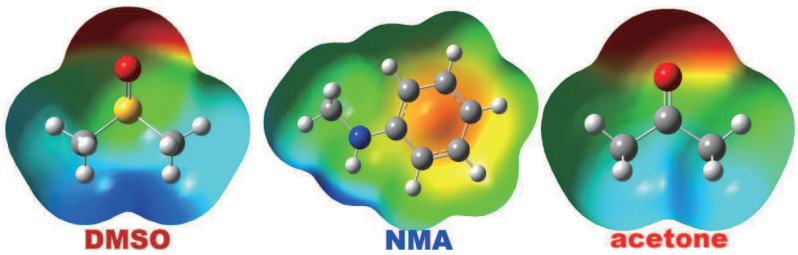

Figure 1: The molecular electrostatic potential (MEP) map of DMSO, NMA and acetone.

3.1.2 The influence of polarity of solvent on hydrogen bond

As shown in Fig. 2, for complex I, the hydrogen bond N_1-$H_1\cdots O_1$ lengthens from acetone solvent (2.065Å) to cyclohexane solvent (2.082Å), which indicates that the intermolecular hydrogen bond is weakened in cyclohexane solvent. Compared with complex I, the hydrogen bond N_1-$H_1\cdots O_1$ of complex II increases to 1.921Å in DMSO solvent. This change demonstrated that the N_1-$H_1\cdots O_1$ hydrogen bond is weakening from DMSO to acetone in ground state.

In order to get a deeper insight into the N_1-$H_1\cdots O_1$ hydrogen bond of complexes I and II in different solvents, the AIM theory of Bader was carried out by the B3LYP/6-311++G(d,p) level. Table 1 list the data of Laplacian of the electron density ($\nabla^2\rho$), electron

Table 1: The Laplacian of the electron density ($\nabla^2\rho$), electron density (ρ) at the hydrogen bond critical point (H-BCP) and the energy of the hydrogen bond (EHB) of complexes I and II in different solvents.

	Complex I/ acetone	Complex I/ cyclohexane	Complex II/ DMSO	Complex II/ cyclohexane
ρ(r)	0.0184	0.0181	0.0258	0.0241
$\nabla^2\rho$(r)	0.0697	0.0669	0.0976	0.0927
E/kj·mol^{-1}	-16.1	-15.6	26.3	24.1

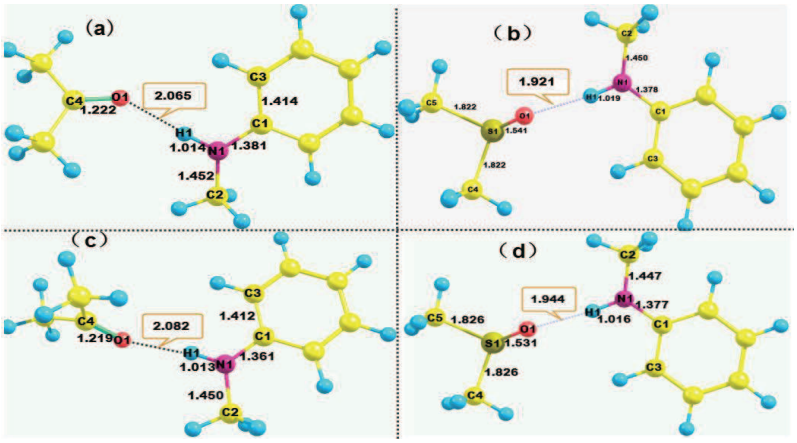

Figure 2: The optimized geometric structures of complexes in different solvents in S_0 state: (a) Complex I in acetone solvent. (b) Complex II in DMSO solvent. (c) Complex I in cyclohexane solvent. (d) Complex II in cyclohexane solvent. Some important bond lengths are labeled.

density (ρ) at the hydrogen bond critical point (H-BCP) and the energy of the hydrogen bond (EHB). According to the topological analysis of the electron density, ρ is used to describe the strength of a bond. And a higher number of ρ indicates a stronger hydrogen bond. Moreover, Hunt and co-workers have proposed the different sets of hydrogen bonding criteria and types [21]. If the Laplacian of the electron density $\nabla^2\rho$ and the electron densities ρ for H$\cdots$Y contact in the range of 0.024-0.139 a.u. and 0.002-0.035 a.u. respectively, it shows that H$\cdots$Y contact is hydrogen bond.

As shown in Table 1, for complex I, the value of the electron density ρ for the intermolecular hydrogen bond N_1-$H_1\cdots O_1$ in acetone and cyclohexane solvents are 0.0184 and 0.0181 a.u respectively. And the Laplacian of the electron density $\nabla^2\rho$ of the intermolecular hydrogen bond N_1-$H_1\cdots O_1$ in acetone and cyclohexane solvents are 0.0697 and 0.0669 a.u respectively. These values are all within the proposed typical range of the hydrogen bond. It can be found that the electron density ρ of hydrogen bond N_1-$H_1\cdots O_1$ in cyclohexane solvent is smaller than that in acetone solvent. This suggests that the intermolecular hydrogen bond N_1-$H_1\cdots O_1$ is stronger with the polarity of solvent stronger. In addition, the ρ of complex I in acetone solvent is smaller than the ρ of complex I in DMSO solvent. This indicated that the hydrogen bond in DMSO solvent is stronger. This

Table 2: The Laplacian of the electron density ($\nabla^2\rho$), electron density (ρ) at the hydrogen bond critical point (H-BCP) and the energy of the hydrogen bond (EHB) of complexes I and II in the S_1 state.

		Complex I/acetone	Complex II/DMSO
S_1 state	ρ(r)	0.0131	0.0389
	$\nabla^2\rho$(r)	0.0476	0.1385
	E/kjomol-1	-10.5	-47.4

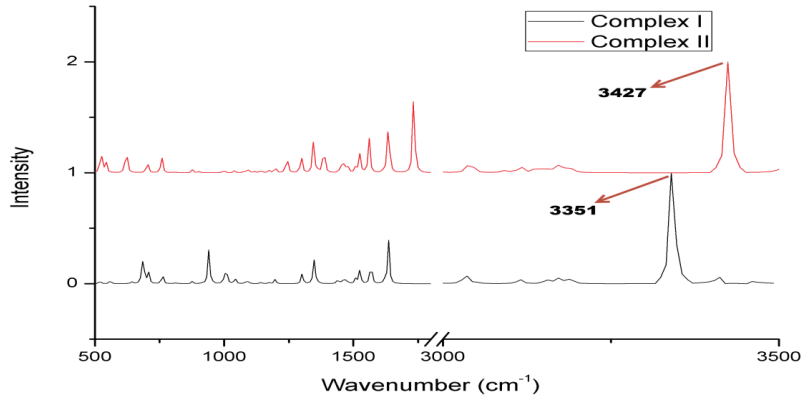

Figure 3: The infrared spectra of complexes I and II in ground state.

is in consistence with the results revealed by Nibbering *et al.* [14].

In order to delineate the change of the intermolecular hydrogen bonding, the infrared spectra of complexes I and II are provided in Fig. 3. As shown in Fig. 3, for complex I, the stretching absorption peak of N1-H1 is located at 3427 cm^{-1} and is in good agreement with the experimental result (3405 cm^{-1}) [14]. For complex II, the N_1-H_1 stretching vibration frequency (3351 cm^{-1}) is smaller than it of complex I and is also in good agreement with the experimental result (3330 cm^{-1}) [14]. This indicates the intermolecular hydrogen bond in complex II is stronger than the hydrogen bond in complex I.

3.2 The nature of hydrogen bond in the S_1 state

Fig. 4 shows the optimized geometric structures of complexes I and II in the S_1 state. The functional groups related to the formation of intermolecular hydrogen bonds of complexes I and II are labeled with bond lengths in excited state. For complex I, the hydrogen bond $N_1\cdots H_1$-O_1 increase from 2.065 Å in ground state to 2.200 Å in the S_1 state, which indicates the intermolecular hydrogen bond $N_1\cdots H_1$-O_1 is weakened upon photoexcitation. Differently, for complex II, the hydrogen bond $N_1\cdots H_1$-O_1 is enhanced from 1.921 Å to 1.751 Å in the S_1 state. The AIM analysis also was performed to confirm this change upon photoexcitation. As shown in Table 2, for complex I, the value of the electron density ρ for the intermolecular hydrogen bond N_1-$H_1\cdots O_1$ is 0.0131 a.u in the S_1 state, which is smaller than it in the ground state (0.0184 a.u). The Laplacian of the

Table 3: The calculated electronic excitation energies (nm) and corresponding oscillator strengths (in Parenthesis) of complexes I and II. The orbital transitions mainly responsible for the $S_0 \rightarrow S_1$ excitation are also listed.

	Complex I	Complex II
S_1	488 (0.002)	329 (0.102)
	HOMO→LUMO 99.6%	HOMO→LUMO 97.8%
S_2	387 (0.002)	293 (0.006)
S_3	302 (0.000)	270 (0.003)
S_4	286 (0.100)	267 (0.004)
S_5	270 (0.022)	261 (0.013)
S_6	250 (0.287)	260 (0.324)

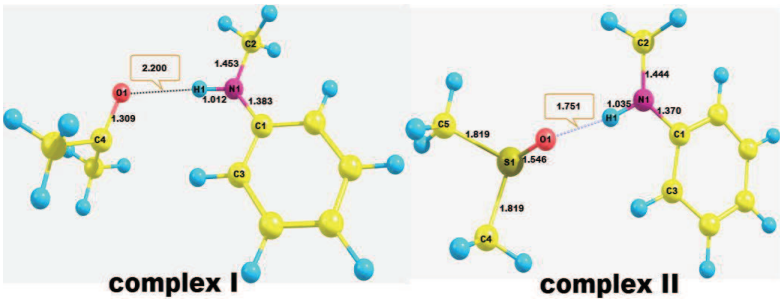

Figure 4: The optimized geometric structures of complexes I and II in the S_1 state. Some important bond lengths are labeled.

electron density $\nabla^2\rho$ of the intermolecular hydrogen bond N_1-$H_1\cdots O_1$ (0.0476 a.u) in the S_1 state is also smaller than it in the ground state (0.0697 a.u). This indicated that the intermolecular hydrogen bond N_1-$H_1\cdots O_1$ is weakened upon photoexcitation. Although the electron density ρ and Laplacian of the electron density $\nabla^2\rho$ of the intermolecular hydrogen bond are very small in the S_1 state, these values are both within the proposed typical range of the hydrogen bond. Differently, the electron density ρ (0.0389) and the Laplacian of the electron density $\nabla^2\rho$ (0.1385) of complex II in the S_1 state are both bigger than them in the ground state. In addition, the energy of intermolecular hydrogen bond N_1-$H_1\cdots O_1$ is increase from 26.3 kj·mol^{-1} in the ground state to 47.4 kj·mol^{-1} in the S_1 state. Therefore, the intermolecular hydrogen bond N_1-$H_1\cdots O_1$ of complex II is strengthened in the S_1 state.

The electronic excitation energies, oscillator strengths and frontier molecular orbitals transition for the first six excited states of complexes I and II are provided in Table 3. In this work, we focus on the S_1 state, a fluorescent state. For the complexes I and II, the electronic excitation energies of the S_1 state are 484 and 329 nm respectively. It can be found that the electronic excitation energy of complex I apparently changes compared to it of complex II. That is to say, the strength of intermolecular hydrogen bond N_1-$H_1\cdots O_1$ has much influence on the electronic absorption spectra.

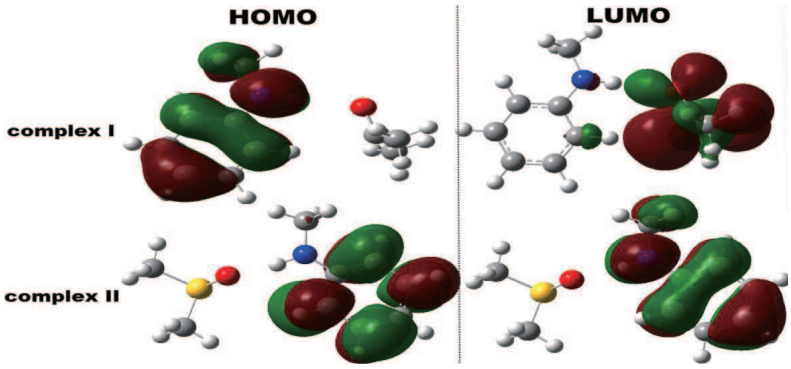

Figure 5: Frontier molecular orbital (MOs) with the highest weigh of contribution on S_1-S_0 transition of complexes I and II.

The frontier molecular orbital are carried out to obtain information regarding the electron density of the complexes I and II [23]. The analysis of molecular orbital can provide insight into the nature of the excited states. According to the data provided in Table 3, the S_1 states of complexes I and II are all correspond to the transition from the highest occupied molecular orbital (HOMO) to the lowest unoccupied molecular orbital (LUMO). Therefore, only the frontier molecular orbital HOMO and LUMO of complexes I and II are shown in Fig. 5. For complex I, it is noted that the electron densities of HOMO are strictly localized on the NMA moiety whereas that of LUMO are localized on the acetone moiety. That is to say, the S_1 state of complex I is a charge transfer (CT) state. This can be used to explain the weakening of the intermolecular hydrogen bond N_1-$H_1\cdots O_1$ upon photoexcitation. Differently, for complex II, the electron density of N_1-H_1 increases obviously after the HOMO→LUMO transition, this indicated the enhancing of hydrogen bond upon photoexcitation.

4 Conclusion

In this work, the intermolecular hydrogen bond N_1-$H_1\cdots O_1$ of complexes I and II both in the ground and the excited S_1 states are discussed in detail. The ESP model demonstrates the conformations of complexes I and II are reasonableness. According to the bond length and AIM analysis, it can be found that the N_1-$H_1\cdots O_1$ hydrogen bonds both of complexes I and II are weakening from DMSO to acetone in ground state. The N_1-$H_1\cdots O_1$ hydrogen bond of complex I in acetone solvent is apparent stronger than that in cyclohexane solvent. Therefore, the N_1-$H_1\cdots O_1$ hydrogen bond is stronger with the polarity of solvent stronger. In addition, the infrared spectra are in good agreement with the experiment data. Upon photoexcitation, the intermolecular hydrogen bond N_1-$H_1\cdots O_1$ both of complex I is weakened whereas that of complex II is strengthened. The frontier molecular orbital analysis illustrated that the S_1 state of complex I is a CT state and it of complex II is a LE state. Therefore, the enhancing of the hydrogen bond of complex II upon pho-

toexcitation is attributed to the electron density of N_1-H_1 increases obviously after the HOMO→LUMO transition. The analysis of molecular orbital also support the results that the intermolecular hydrogen bond N_1-$H_1\cdots O_1$ of complex I is weakened whereas it of complex II is enhanced.

Acknowledgments. This work was supported by the National Natural Science Foundation of China (Grant No. 11274096), Innovation Scientists and Technicians Troop Construction Projects of Henan Province of China (Grant No. 124200510013) and Science and Technology Research Key Project of Education Department of Henan Province of China (Grant No. 13A140690).

References

[1] Y. F. Liu, J. X. Ding, R. Q. Liu, D. H. Shi and J. F. Sun, J. Photochem. Photobiol. A-Chem., 201 (2009) 203.
[2] T. S. Pandian, S. J. Cho, J. Kang and J. Org. Chem., 78 (2013) 12121.
[3] M. P. Printz, H. P. Williams, L. C. Craig, Proceedings of the National Academy of Sciences of the United States of America, 69 (1972) 378.
[4] H. L. Ronkko, H. Knuuttila, M. Haukka and T. T. Pakkanen, Inorg. Chim. Acta, 376 (2011) 687.
[5] H. W. Tseng, J. Q. Liu, Y. A. Chen, C. M. Chao, K. M. Liu, C. L. Chen, T. C. Lin, C.H. Hung, Y. L. Chou, T.C. Lin, T.L. Wang and P.T. Chou, J. Phys. Chem. Lett., 6 (2015) 1477.
[6] R. L. Wu, Q. Ji, B. Kong and X. Z. Yang, Sci. China Ser. B-Chem., 51 (2008) 736.
[7] Z. Zhang, C. B. Post and D. L. Smith, Biochemistry, 35 (1996) 779.
[8] C. Chen, W. Z. Li, Y. C. Song, L. D. Weng and N. Zhang, Bull. Korean Chem. Soc., 33 (2012) 2238.
[9] S. Chowdhuri and A. Chandra, J. Phys. Chem. B, 110 (2006) 9674.
[10] Z. S. Derewenda and L. Lee, U. Derewenda, J Mol Biol, 252 (1995) 248.
[11] K. Eskandari and C. Van Alsenoy, J. Comput. Chem., 35 (2014) 1883.
[12] Y. F. Liu, J. X. Ding, D. H. Shi and J. F. Sun, J. Phys. Chem. A, 112 (2008) 6244.
[13] G. J. Zhao and K. L. Han, Accounts Chem. Res., 45 (2012) 404.
[14] M. Prémont-Schwarz, S. Schreck, M. Iannuzzi, E. T. J. Nibbering, M. Odelius and P. Wernet, J. Phys. Chem. B, (2015).
[15] R. Ahlrichs, M. Bär, M. Häser, H. Horn and C. Kölmel, Chem Phys Lett, 162 (1989) 165.
[16] A. D. Becke, J. Chem. Phys., 98 (1993) 5648.
[17] B. G. Johnson, P. M. Gill and J. A. Pople, J. Chem. Phys., 98 (1993) 5612.
[18] R. Krishnan, J. S. Binkley, R. Seeger and J. A. Pople, J. Chem. Phys., 72 (1980) 650.
[19] P. C. Hariharan, J. A. Pople, Theor. Chim. Acta, 28 (1973) 213.
[20] R. F. Bader, Oxford University Press, Oxford Henkelman G, Arnaldsson A, Jónsson H (2006) A fast and robust algorithm for Bader decomposition of charge density. Comput Mater Sci, 36 (1990) 354.
[21] P. A. Hunt, C. R. Ashworth and R. P. Matthews, Chem Soc Rev, 44 (2015) 1257.
[22] P. A. Hunt, B. Kirchner and T. Welton, Chemistry (Weinheim an der Bergstrasse, Germany), 12 (2006) 6762.
[23] V. Lemaur, M. Steel, D. Beljonne and J. L. Bredas, J. Cornil, J. Am. Chem. Soc., 127 (2005) 6077.